Environmental Science & Technology Letters

Letter

pubs.acs.org/journal/estlcu

A Fluence-Based Method for the Direct Comparison of Photolysis Kinetics under Variable Light Regimes

Maya L. Wei-Haas and Yu-Ping Chin*

School of Earth Sciences, The Ohio State University, 125 South Oval Mall, Columbus, Ohio 43210, United States

Supporting Information

ABSTRACT: Chemical actinometers are traditionally used to account for photochemical experiments conducted under different light regimes (simulated vs natural; also seasonal, daytime, cloud cover, and latitude changes). Their many limitations and the lack of a universally applicable actinometer demand development of a new approach for studying environmentally relevant photochemical processes in sunlight. We suggest the use of fluence-based rate constants (converted to time-based rate constants and half-lives with irradiance normalization), using a data-logging radiometer to track the accumulated dose of UVA and UVB radiation. Our results suggest that this method can effectively account for minor changes in cloud cover and sun angle in the photolysis of *p*-nitroanisole/pyridine and *p*-nitroacetophenone/pyridine. The greatest error is caused by factors (e.g., dense cloud cover, extreme sun angles, and changes in ozone) that affect relative UVA and UVB fluence. We believe that this simple and elegant method serves as an important bridge between laboratory and field-based environmental photochemistry experiments.

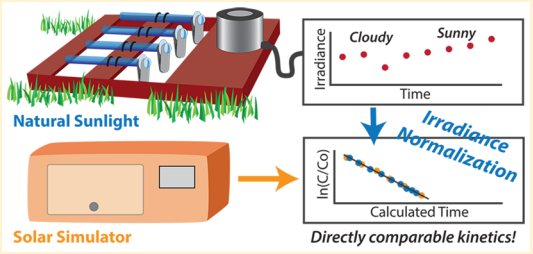

INTRODUCTION

Quantification of photon flux is an integral step in studying environmental photochemical reactions. In the environmental photochemistry field, chemical actinometry is the most common method to account for the naturally high variability of photon flux that results from changes in cloud cover and spatiotemporal influences on sun angle.[1−3] Using this method, the direct photolysis of an actinometer (a compound with a known quantum yield or ϕ_A) is monitored at a specific wavelength. By simultaneously conducting experiments with the actinometer and analyte, the latter's quantum yield (ϕ_B) can be calculated via direct comparison of degradation rates.[1,3]

There are many desirable traits for an actinometer, which makes it challenging to identify one that can be universally applied. Actinometer qualities of importance include high stability in the dark and a ϕ_A that is independent of temperature, wavelength, and concentration.[2] Chemical actinometers must also degrade to inert photoproducts to limit side reactions and analytical interference.[2] Finally, chemical actinometers ideally exhibit a half-life similar to that of the target analyte to account for changes in light intensity throughout the experiment.[3]

Because all of these traits are rarely met by a single actinometer, the accuracy and environmental applicability of the target analyte ϕ_B are often limited. Few actinomteters exhibit ϕ_A that are independent of wavelength (λ), resulting in a wavelength-specific analyte ϕ_B. Given this limitation, the comparison of ϕ_B, calculated at different wavelengths across multiple studies, is difficult to accomplish. Extrapolation of ϕ_B measured at a single wavelength to environmentally relevant values or differing light regimes is challenging to near impossible.

Although actinometers with a variety of half-lives exist, we are unaware of any that are currently used to study compounds with long half-lives that necessitate full to multiday exposure periods. Thus, many studies involving the photolysis of these slowly reacting analytes typically report reaction rate constants rather than ϕ_B, making it difficult to compare experiments conducted under different light regimes.[4−8] Finally, the necessary simultaneous exposure of actinometer and target compounds is particularly challenging to accomplish in remote field locations, where supplies and analytical facilities are often limited.

These limitations demand the development of a more robust means of studying photochemical kinetics that allows direct comparison between experiments conducted under varying light regimes (simulated and natural sunlight). In this study, we investigate the use of a data-logging radiometer equipped with a UVA+UVB detector [~280−380 nm (Figure S1 of the Supporting Information)] to calculate *fluence-based* rate constants, which can be easily converted into time-based rate constants or half-lives at chosen irradiance intensities. While time-based rate constants vary with radiant exposure, fluence-based rate constants are independent of light regime. Fluence (i.e., dose) is the radiant exposure for the analyte, while fluence rate is similar to irradiance. For a more in-depth discussion of

Received: January 27, 2015
Revised: May 30, 2015
Accepted: June 1, 2015
Published: June 1, 2015

DOI: 10.1021/acs.estlett.5b00130
Environ. Sci. Technol. Lett. 2015, 2, 183−187

these terms, refer to Bolton and Linden.[9] We acknowledge that the use of physical means to measure photon flux is not a new method and the use of fluence-based rate constants is common in the UV disinfection field.[9−12] Yet this method is unexplored in the field of environmental photochemistry and little is known about its applicability for natural sunlight. We believe that this simple and elegant method will serve as an important bridge between laboratory and field experiments and support wider applicability of experimental results gathered in diverse environments and under variable light regimes.

MATERIALS AND METHODS

Chemicals. To test this method with compounds possessing a wide range of half-lives, we used the adjustable actinometers, *p*-nitroanisole (PNA) and *p*-nitroacetophenone (PNAP).[2] Stock solutions of PNA and PNAP were prepared in HPLC grade acetonitrile (ACN) obtained from Fisher Scientific (Hampton, NH). The following working solutions were prepared in Milli-Q water: PNA only (10^{-5} M), PNA (10^{-5} M) with pyridine (5×10^{-3} M), or PNAP (10^{-5} M) with pyridine (6×10^{-2} M). All water was ultrapure and deionized using a Milli-Q water system (EMD Millipore, Billerica, MA). PNA (>98%) was obtained from Tokyo Chemical Industry (TCI, Portland, OR). PNAP (98%) and HPLC grade pyridine (99.9%) were obtained from Sigma-Aldrich (Milwaukee, WI).

Photolysis Experimental Setup. The compounds were photolyzed in quartz phototubes (1.12 cm path length). We collected seven time points per experiment, with duplicates at each time point. Dark controls were run concurrently at similar temperatures. Photodegradation experiments using each actinometer were conducted in our solar simulator (Suntest CPS+, Atlas, Mount Prospect, IL) over a temperature range of 24−27 °C, unless otherwise noted.

For natural sunlight experiments, phototubes were secured to a black anodized aluminum rack attached to a leveled crate ∼12 in. above the ground. Experiments were conducted in Columbus, OH (40°00′N, 83°01′W), during October−November 2013 and April−June 2014 and at a site near the Toolik Field Station, North Slope, AK (68°38′N, 149°36′W), during July−August 2014. Additional details concerning field setups and weather conditions for each experiment are included in the Supporting Information (section S5.3 and Table S3).

Analytical Instrumentation. Irradiance was monitored using the PMA2100 data-logging radiometer coupled to a PMA2107 UVA+UVB Teflon-coated photodiode detector (Solar Light Co., Glenside, PA). Actinometer samples were analyzed on either a Waters (Milford, MA) 1515 HPLC system with a 2487 dual absorbance detector or an Agilent (Santa Clara, CA) 1100 HPLC system with a diode array detector. For both systems, the mobile phase was a 50:50 acetonitrile/Milli-Q water mixture (flow rate of 1 mL/min). Peaks were monitored at 316 nm.

Calculations and Correction Factors. The PMA2107 has an angular response that closely follows a cosine function (Figure S2 of the Supporting Information). As such, each irradiance measurement was corrected for changes in the solar zenith angle, which was calculated at 1 min intervals using the National Renewable Energy Laboratory (NREL) Measurement and Instrumentation Data Center (MIDC) solar position algorithm (uncertainties of ±0.0003).[13] Earth orientation parameters for calculations were obtained from the International Earth Rotation and Reference System Service (IERS).[14] Because the irradiance measurement error drastically increases at large zenith angles (Figure S2 of the Supporting Information), we limited sample exposure to zenith angles of approximately <70° (error of approximately <10%). The only exceptions to the latter parameter are results from experiments conducted during late October and November, intended to test the effects of a low sun angle (for parameters, see Tables S1 and S2 of the Supporting Information).

The logging radiometer recorded the average irradiance at 1 min intervals. This value was then multiplied by the logging interval (in seconds) to convert to dose per minute. The accumulated dose was calculated for each time point as the sum of doses per minute since the initial exposure. A fluence-based pseudo-first-order rate constant (k_f in units of square centimeters per joule) was then calculated by using the absolute value of the slope for the plot, ln(C/Co), versus the accumulated dose (joules per square centimeter). This rate constant can be used to calculate the analyte half-life ($t_{1/2}$) by multiplying a user-defined irradiance value [irradiance normalization factor (INF)]. Alternatively, a time-based rate constant may be calculated by normalizing the accumulated dose for a specific time point to the INF, which yields the calculated exposure time. A spreadsheet with example calculations is available in the Supporting Information.

The INF may be any value of irradiance (measured or calculated) that suits the experimental design. We calculated half-lives based on both the average natural sunlight irradiance during sample exposure for each experiment (INF_{ns}) (range of 2.61−5.77 mW cm^{-2}) and a value approximating irradiance measured in our solar simulator (INF_{ss}) (6.0 mW cm^{-2}). Because the intensity of this simulated light spatially varies (5.8−6.5 mW cm^{-2}), the chosen value for INF_{ss} produces the most comparable indoor and outdoor degradation rates.

RESULTS AND DISCUSSION

We tested the use of the fluence-based rate under a variety of outdoors conditions with the PNA/pyridine, PNA only, and PNAP/pyridine chemical actinometers, which exhibited half-lives ranging from approximately 20 min to 8 h under simulated sunlight. The values of k_f for PNA only and PNA/pyridine experiments conducted in Columbus, OH, under natural sunlight were statistically identical under both full sun and partly cloudy conditions (Table S3 of the Supporting Information). Furthermore, INF_{ss}-corrected (i.e., solar simulator irradiance intensity, 6 mW cm^{-2}) half-lives for natural sunlight experiments are in excellent agreement with measured values under simulated light [1−6% for PNA only and 2−8% for PNA/pyridine (see Figure 1A, B)]. In contrast, analyte half-lives calculated using the average natural sunlight irradiance during sample exposure (i.e., INF_{ns}) deviated 2−132% from the half-lives measured in the solar simulator (Figure 1A, B). This large range simply reflects the wide range of INF_{ns} measured during sample exposure under natural sunlight as noted earlier.

The INF_{ss}-corrected half-life for the PNAP/pyridine outdoor experiment is also comparable to measurements under simulated light ($t_{1/2} \sim 8$ h), but only when both experiments were conducted at similar temperatures (Figure 1C). Notably, this observation runs contrary to the previously reported temperature independence for PNAP/pyridine photolysis by Dulin and Mill.[2]

Significant deviations in both fluence-based rate constants and INF_{ss}-corrected half-lives (>10%) occurred for experiments conducted outdoors under dense cloud cover and low sun angle (Figure 1) and are discussed in more depth in the following

DOI: 10.1021/acs.estlett.5b00130
Environ. Sci. Technol. Lett. 2015, 2, 183−187

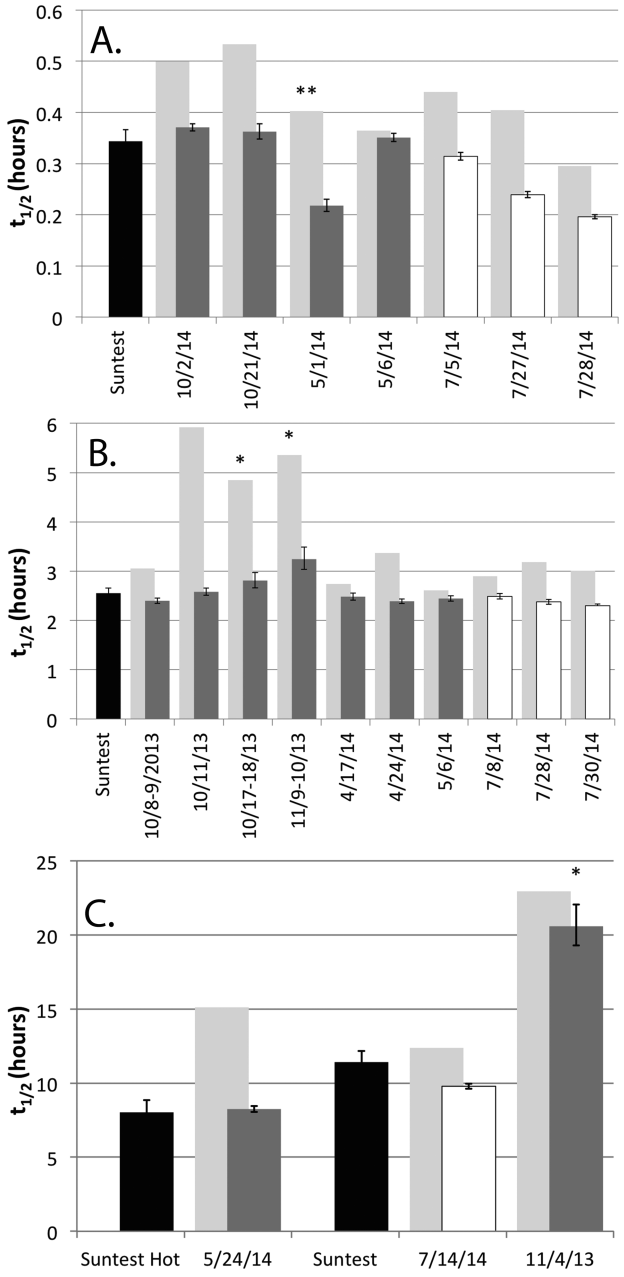

Figure 1. Comparison of half-lives for PNA/pyridine (A), PNA only (B), and PNAP/pyridine (C) actinometers under simulated (black bars) and natural light. For experiments under natural light, half-lives are calculated using the INF_{ss} in Ohio (dark gray) and Alaska (white). For comparison, half-lives normalized with the INF_{ns} (light gray) are displayed for each natural sunlight experiment. Two asterisks denote exposure under dense cloud cover. One asterisk denotes exposure during the late fall with a low sun angle.

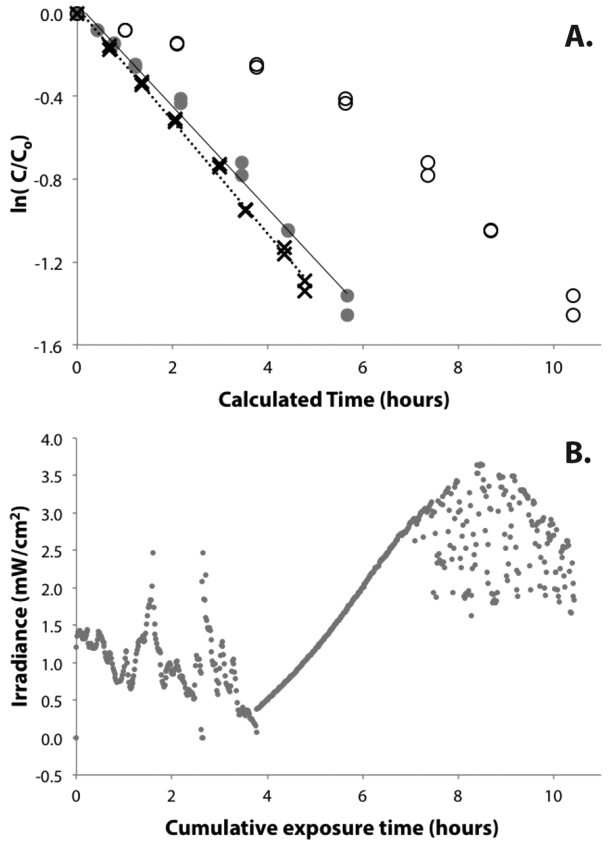

Figure 2. Comparison of PNA degradation kinetics (A) measured under natural sunlight (October 17 and 18) to the solar simulator, demonstrating the efficacy of INF normalization. Irradiance variation measured during sample exposure in natural sunlight is displayed in panel B. The uncorrected PNA data (○) measured in natural sunlight are nonlinear with a half-life significantly longer than that of the experiment conducted under simulated light (×). However, after INF_{ss} normalization (gray circles), the results of the degradation experiment follow first-order kinetics and align more closely with the solar simulator data. The remaining difference in slope between experiments conducted under simulated and natural light likely originates from the low sun angles during the outdoor experiment.

sections. Even for these experiments, however, deviations from first-order kinetic behavior due to changes in sunlight intensity were successfully corrected using INF normalization (either INF_{ns} or INF_{ss}) rather than uncorrected time (Figure 2).

In addition to the aforementioned experiments exposed under dense clouds and low sun angles, uncorrected PNA only and PNAP/pyridine degradation kinetics displayed the most frequent deviations from first-order kinetics. This is likely due to their slower kinetics, which resulted in exposure to a range of irradiance intensities over the course of a single experiment. Because the half-life of the PNA/pyridine degradations is short (~30 min outdoors at 40°N), the irradiance intensity at peak sun angles in June was relatively constant and similar to those in our solar simulator. INF normalization in these experiments produced only small changes in the rate constant of the analytes, although this method is still useful in these instances as it reduces the need to conduct simultaneous actinometer experiments. Nonetheless, our method is most beneficial for compounds that exhibit slow photodegradation kinetics.

Overall, these results indicate that the use of fluence-based rate constants and INF normalization is temporally robust and capable of correcting for changes in irradiance due to sun angle (>20°) and minor cloud cover (Figure 1). Moreover, this method successfully corrects for any nonlinearity in the degradation kinetics for outdoor experiments resulting from variable irradiance intensity.

Effects of Dense Cloud Cover and Low Sun Angles. Although our irradiance normalization method can largely account for minor changes in cloud cover and sun angle, we observed several notable conditions that result in deviations from the predicted half-lives. Degradation experiments for PNA/pyridine conducted under continuous, dense cloud cover resulted in an INF_{ss}-corrected half-life that was considerably

DOI: 10.1021/acs.estlett.5b00130
Environ. Sci. Technol. Lett. 2015, 2, 183−187

lower than values measured under simulated sunlight (Figure 1A and Table S3 of the Supporting Information). Conversely, the corrected half-lives for PNAP/pyridine and PNA only experiments conducted during late October and November were >10% longer than those measured in the solar simulator (Figure 1B, C and Table S3 of the Supporting Information).

These anomalous results may be explained by the different sensitivities of the radiometer and the chemical actinometers to changing solar spectra. The PMA2107 detector used for these experiments measures bulk UVA+UVB irradiance (Figure S1 of the Supporting Information), while the analytes primarily absorb UVB or shorter wavelengths (λ_{max} = 315 and 275 nm, respectively) and minimally absorb in the UVA region (λ > 330 nm) (Figure S3 of the Supporting Information).

Clouds result in Mie scattering of both UVA and UVB irradiance, but because UVB light is scattered by the atmosphere under all conditions, cloud cover results in relatively greater UVA scattering.[15] Consequently, the ratio of UVB to UVA+UVB (i.e., UV_{tot}) irradiance under dense cloud cover is greater relative to clear skies, resulting in a larger fluence-based rate constant and thus shorter than expected INF_{ss}-normalized half-lives.

The observed increasing half-lives for PNAP/pyridine and PNA only experiments conducted during late October and November may also result from changes in the UVB/UV_{tot} ratio (Figure 2). A low sun angle (high solar zenith angle) results in an effect that is opposite to that of cloud cover, whereby Rayleigh scattering influences UVB more strongly than UVA (Figures S4 and S5 of the Supporting Information).[3,15] This results in a lower UVB/UV_{tot} ratio, a smaller fluence-based rate constant, but a longer INF_{ss}-normalized half-life (Figures 1 and 2). However, it is important to note that other factors such as lower temperatures may also play a role in experiments conducted during fall and winter. As noted above, faster kinetics was observed for PNAP/pyridine at >33 °C (Figure 1C). Because many organic micropollutants that undergo direct photolysis in sunlight possess labile chromophores that absorb UVB light, these problems may largely be overcome by using a UVB only radiometer probe.

Latitude, Elevation, and Ozone Effects. We examined how changes in latitude and altitude affect the fluence-based rate constants by conducting experiments at the Toolik Field Station (TFS), North Slope, AK (68°N, 721 m). For PNA only experiments, fluence-based rate constants measured at TFS (0.0129−0.0140 $cm^2\ J^{-1}$) were comparable to values measured in Columbus, OH (0.0124−0.0134 $cm^2\ J^{-1}$) (Figure 1B). Furthermore, the INF_{ss}-corrected half-lives for PNA only experiments measured at TFS fell within 10% of half-lives measured under simulated and natural sunlight in Columbus, OH (Figure 2B). The PNAP/pyridine experiment had an INF_{ss}-corrected half-life shorter than the solar simulator-measured value (∼14% deviation).

The UVB/UV_{tot} ratio decreases slightly with latitude (Figure S5 of the Supporting Information) but increases with elevation[15] (TFS is ∼500 m higher than Columbus, OH). These changes may influence the fluence-based rate constants, resulting in lower corrected half-lives observed for most actinometer experiments conducted in Alaska compared to Ohio (Figure 1B, C). However, these differences cannot account for the trending increase in fluence-based rate constants (and decreasing INF_{ss}-corrected half-lives) for repeat PNA/pyridine experiments relative to measurements under simulated light [−9, −30, and −43% (Figure 1A and Table S3 of the Supporting Information)]. Seasonal variability in ozone, which absorbs only UVB light, may be the source of this observed trend.[15] The seasonal variability of ozone is considerably greater in the Arctic than at lower latitudes because of the large seasonal changes in sunlight. In the Arctic, ozone concentrations peak during the dark winter and spring months and steadily decrease through the summer and early fall because of continuous sunlight exposure.[16] Thus, as the ozone concentrations decrease, the UVB/UV_{tot} ratio is expected to increase. However, additional research is necessary to confirm the significance of ozone changes for the use of this method.

Although less distinct, this trend is also apparent in the rate constants and half-lives of PNA only experiments [−3, −7, and −10% half-live differences from solar simulator (Figure 1B)]. It is likely that the longer exposure period for these experiments resulted in "averaging" conditions of relatively higher and lower UVB light, producing analyte half-lives comparable to those of experiments conducted in Ohio.

To roughly test the influences of UVB on INF-normalized half-lives, we obtained UVB measurements (5 min increments) from TFS for each PNA/pyridine experiment.[17] If these values are used in lieu of our PMA2100 measurements for calculations, the difference between corrected half-lives for the July 27 and 28 experiments is only 1%. However, the corrected half-life for the July 5 experiment is over 40% greater than those in late July, suggesting the presence of additional factors that influence the degradation rates. Admittedly, the use of the TFS irradiance data is imperfect because of the long logging interval (5 min) and location of the UVB probe distal to the experimental setup. Furthermore, the PNA/pyridine reaction rate is dependent on the pyridine concentration; thus, variations in the concentration of this reagent (e.g., volatilization) prepared under less than ideal conditions (in a remote field station) considerably influence the quantum yield. Thus, more experimentation is necessary to explore factors influencing INF normalization at high latitudes.

Fluence-Based Rate Constant Limitations. As these deviations demonstrate, the accuracy and reproducibility of fluence-based rate constants rely on the overlap and relative sensitivities of the radiometer spectral range, actinometer absorbance, and solar (simulated or natural) spectra. Ideally, the wavelength range for the radiometer probe and actinometer absorbance would largely overlap. Thus, a radiometer with a wide detection range becomes less practical for correcting irradiance differences.

Another important consideration is that the irradiance magnitude for sunlight measured with a UVB radiometer probe will be lower than that of a UVA+UVB probe, resulting in an overall larger fluence-calculated rate (i.e., fluence-based rate constants measured with the former are not directly comparable to those measured with the latter). Furthermore, as this method relies solely on probe measurements, outside standardization and verification of probe accuracy is necessary.[9] More importantly, periodic testing of method precision should be conducted using a chemical actinometer.

Although it is beyond the scope of this study, comparison of solar simulator- to natural sunlight-determined rate constants must also consider light screening, direct versus indirect photolysis mechanisms, and exposure surface curvature. Details about conversion of measured rates to environmentally relevant conditions can be found in section S5 of the Supporting Information. Furthermore, this study addresses the use of this method for only compounds that degrade via pseudo-first-order

DOI: 10.1021/acs.estlett.5b00130
Environ. Sci. Technol. Lett. 2015, 2, 183−187

kinetics, and more research is necessary for non-first-order kinetics applications.

Overall, our results suggest that fluence-based rate constants are a robust means to correct for irradiance variation due to modest changes in cloud cover and temporal changes in sun angle. Because the photodegradation of many compounds is largely dictated by UVB dose, the use of a UVB only probe (or optical filters permitting only UVB transmission) will likely produce greater precision and accuracy and allow wider applicability of this method to directly compare experiments conducted under a broad range of spatiotemporal and weather conditions (e.g., high latitudes, dense cloud cover, and low sun angles). Furthermore, although this study was limited to compounds that undergo direct photolysis, we believe that this approach can also be used to compare indirect photolysis rate constants measured in both simulated and natural sunlight provided that the experimental design is identical for both irradiance scenarios (section S5.2 of the Supporting Information). These results are particularly significant for slowly degrading compounds and research at remote field stations, where supplies and analytical capacity are limited.

This study serves as a first step in the transition to fluence rather than time-based rate constants for photolysis conducted in natural and artificial sunlight. We acknowledge that continued testing of this method with a wider range of compounds is necessary to shift the time-based rate constants and chemical actinometry paradigm in environmental chemistry. However, we believe that the use of fluence-based rate constants and INF normalization to calculate half-lives allows direct comparison of photodegradation rates measured in natural sunlight to those determined in a solar simulator, thereby allowing us to bridge the gap between laboratory and field studies.

■ ASSOCIATED CONTENT

Supporting Information

A spreadsheet with example calculations and additional information on probe detection, solar spectra, and experimental conditions and considerations. The Supporting Information is available free of charge on the ACS Publications website at DOI: 10.1021/acs.estlett.5b00130.

■ AUTHOR INFORMATION

Corresponding Author

*E-mail: yo@geology.ohio-state.edu. Phone: (614) 292-6953. Fax: (614) 292-7688.

Notes

The authors declare no competing financial interest.

■ ACKNOWLEDGMENTS

This work was supported by the National Science Foundation (NSF) Graduate Research Fellowship awarded to M.L.W.-H. (DGE-0822215) and NSF Grant ARC-1203861. We thank Charles Sharpless (University of Mary Washington, Fredericksburg, VA) for providing the SMARTS solar spectrum data and plot of monthly changes in UVB/UV_{tot} ratio. We also thank Tom Green and Jen Guerard [University of Alaska, Fairbanks (UAF), Fairbanks, AK] for assistance with sample analysis and use of instrumentation at UAF. Arctic UVB data sets and weather conditions were provided by the Toolik Field Station Environmental Data Center.

■ REFERENCES

(1) Montalti, M.; Credi, A.; Prodi, L.; Gandolfi, T. M. *Handbook of photochemistry*, 3rd ed.; Taylor & Francis: Boca Raton, FL, 2006.

(2) Dulin, D.; Mill, T. Development and evaluation of sunlight actinometers. *Environ. Sci. Technol.* **1982**, *16* (11), 815−820 DOI: 10.1021/es00105a017.

(3) Leifer, A. *The kinetics of environmental aquatic photochemistry: Theory and practice*; American Chemical Society: Washington, DC, 1988.

(4) Dimou, A. D.; Sakkas, V. A.; Albanis, T. A. Metolachlor photodegradation study in aqueous media under natural and simulated solar irradiation. *J. Agric. Food Chem.* **2005**, *53* (3), 694−701 DOI: 10.1021/jf048766.

(5) Rayne, S.; Wan, P.; Ikonomou, M. Photochemistry of a major commercial polybrominated diphenyl ether flame retardant congener: 2,2′,4,4′,5,5′-hexabromodiphenyl ether (BDE153). *Environ. Int.* **2006**, *32* (5), 575−585 DOI: 10.1016/j.envint.2006.01.009.

(6) Shih, Y.-H.; Wang, C.-K. Photolytic degradation of polybromodiphenyl ethers under UV-lamp and solar irradiations. *J. Hazard. Mater.* **2009**, *165* (1−3), 34−38 DOI: 10.1016/j.jhazmat.2008.09.103.

(7) Peuravuori, J.; Pihlaja, K. Phototransformations of selected pharmaceuticals under low-energy UVA−VIS and powerful UVB−UVA irradiations in aqueous solutions: The role of natural dissolved organic chromophoric material. *Anal. Bioanal. Chem.* **2009**, *394* (6), 1621−1636 DOI: 10.1007/s00216-009-2816-7.

(8) Chen, L.; Shen, C.; Zhou, M.; Tang, X.; Chen, Y. Accelerated photo-transformation of 2,2′,4,4′,5,5′-hexachlorobiphenyl (PCB 153) in water by dissolved organic matter. *Environ. Sci. Pollut. Res.* **2013**, *20* (3), 1842−1848 DOI: 10.1007/s11356-012-1112-9.

(9) Bolton, J. R.; Linden, K. G. Standardization of methods for fluence (UV dose) determination in bench-scale UV experiments. *J. Environ. Eng.* **2003**, *129* (3), 209−215.

(10) Kuhn, H. J.; Braslavsky, S. E.; Schmidt, R. Chemical actinometry (IUPAC technical report). *Pure Appl. Chem.* **2004**, *76* (12), 2105−2146.

(11) Shemer, H.; Linden, K. Degradation and by-product formation of diazinon in water during UV and UV/H_2O_2 treatment. *J. Hazard. Mater.* **2006**, *136* (3), 553−559 DOI: 10.1016/j.jhazmat.2005.12.028.

(12) Sharpless, C. M.; Linden, K. G. Experimental and model comparisons of low- and medium-pressure hg lamps for the direct and H_2O_2 assisted UV photodegradation of n-nitrosodimethylamine in simulated drinking water. *Environ. Sci. Technol.* **2003**, *37* (9), 1933−1940 DOI: 10.1021/es025814p.

(13) Reda, I.; Andreas, A. Solar position algorithm for solar radiation applications. NREL Report TP-560-34302; National Renewable Energy Laboratory: Golden, CO, 2003.

(14) International Earth Rotation and Reference System Service (IERS); http://iers.org.

(15) Moan, J. Visible light and UV radiation. In *Radiation at Home, Outdoors and in the Workplace*; Persson, B. R., Paakkonen, R., Hellborg, R., Brune, D., Eds.; Scandinavian Science Publisher: Oslo, 2001; pp 69−85.

(16) Fahey, D. W.; Hegglin, M. I. Section 1: Ozone in our atmosphere. In *Twenty Questions and Answers About the Ozone Layer: 2010 Update*; World meteorological organization global ozone research and monitoring project Report 52; 2010; pp 10−11.

(17) Environmental Data Center Team. Meteorological Monitoring program at Toolik, Alaska; Institute of Arctic Biology, University of Alaska, Fairbanks, Fairbanks, AK (http://toolik.alaska.edu/edc/abiotic_monitoring/data_query.php).